Photocatalytic and Chemoselective H/D Exchange at α-thio C(sp^3)-H Bonds

Riku Ogasahara,‡ Miyu Mae,‡ Yuki Itabashi, Kei Ohkubo, Keisuke Matsuura, Hyoga Shimizu, Kazuho Ban, Masaki Togami, Taro Udagawa, Hiroyoshi Fujioka, Mako Kamiya, Shuji Akai, Yoshinari Sawama*

Riku Ogasahara – Graduate School of Pharmaceutical Sciences, Osaka University, 1-6 Yamada-oka, Suita, Osaka 565-0871, Japan

Miyu Mae – Graduate School of Pharmaceutical Sciences, Osaka University, 1-6 Yamada-oka, Suita, Osaka 565-0871, Japan

Yuki Itabashi – Institute for Open and Transdisciplinary Research Initiatives (OTRI), Osaka University, Yamada-oka 1-6, Suita, Osaka, 565-0871, Japan

Kei Ohkubo – Institute for Open and Transdisciplinary Research Initiatives (OTRI), Osaka University, Yamada-oka 1-6, Suita, Osaka, 565-0871, Japan

Keisuke Matsuura – Graduate School of Pharmaceutical Sciences, Osaka University, 1-6 Yamada-oka, Suita, Osaka 565-0871, Japan

Hyoga Shimizu – Graduate School of Pharmaceutical Sciences ,Osaka University, 1-6 Yamada-oka, Suita, Osaka 565-0871, Japan

Kazuho Ban – Graduate School of Pharmaceutical Sciences, Osaka University, 1-6 Yamada-oka, Suita, Osaka 565-0871, Japan

Masaki Togami – Graduate School of Pharmaceutical Sciences, Osaka University, 1-6 Yamada-oka, Suita, Osaka 565-0871, Japan

Taro Udagawa – Department of Chemistry and Biomolecular Science, Faculty of Engineering, Gifu University, 1-1 Yanagido, Gifu 501-1193, Japan

Hiroyoshi Fujioka – Department of Life Science and Technology, Institute of Science Tokyo, 4259 Nagatsuta, Midori-ku, Yokohama, Kanagawa 226-8501, Japan

Mako Kamiya – Department of Life Science and Technology, Institute of Science Tokyo, 4259 Nagatsuta, Midori-ku, Yokohama, Kanagawa 226-8501, Japan. The Research Center for Autonomous Systems Materialogy (ASMat), Institute of Innovative Research (IIR), Institute of Science Tokyo, 4259 Nagatsuta, Midori-ku, Yokohama, Kanagawa 226-8501, Japan

Shuji Akai – Graduate School of Pharmaceutical Sciences, Osaka University, 1-6 Yamada-oka, Suita, Osaka 565-0871, Japan.

Yoshinari Sawama – Graduate School of Pharmaceutical Sciences Osaka University, 1-6 Yamada-oka, Suita, Osaka 565-0871, Japan. Deuterium Science Research Unit, Center for the Promotion of Interdisciplinary Education and Research, Kyoto University, Yoshida, Sakyo-ku, Kyoto 606-8501, Japan

‡ equally contributed

KEYWORDS. deuteration; deuterium oxide; photocatalyst; α-thio C(sp^3)-H bond, selectivity

ABSTRACT: Deuterated compounds used in drug discovery and live-cell imaging have recently gained the attention of various scientific fields. Although hydrogen-deuterium (H/D) exchange reactions are straightforward deuteration methods, achieving perfect chemoselectivity is challenging. We report the highly chemoselective deuteration of α-thio C(sp^3)-H bonds using a thioxanthone or anthraquinone organic photocatalyst bearing an aromatic ketone skeleton and D_2O as an

inexpensive deuterium source under 390 nm irradiation. Notably, deuterium incorporation at the α-positions of O/N atoms, benzylic positions, and aromatic rings was not observed. The present chemoselectivity was accomplished via a single electron transfer mechanism between the photocatalyst and S-containing substrates, as proven by laser-induced time-resolved transient absorption spectroscopic measurements. Furthermore, the proposed deuteration method could be applied to various S-containing substrates including pharmaceuticals and biologically active compounds with high regioselectivities. The available deuterated compounds as novel deuterated alkylation reagents for future drug discovery and as materials for Raman imaging were also demonstrated.

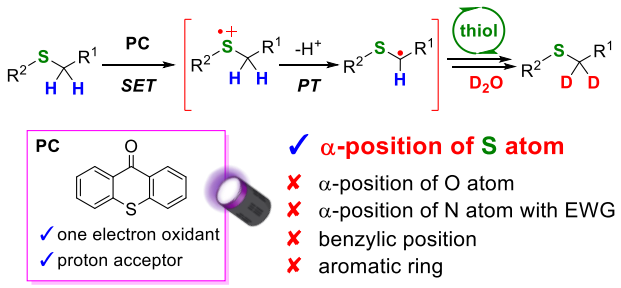

INTRODUCTION

Deuterium (D) is a stable and nonradioactive isotope of hydrogen (H), and deuterated compounds can be handled in a standard laboratory without special permission, handling licenses, or radiation safety measures. Compared to the synthesis of other isotopes (^{13}C, ^{15}N, etc.)-substituted compounds, the incorporation of deuterium (H/D) exchange reaction) has numerous advantages in terms of ease, speed, and lower cost. Therefore, deuterated compounds have recently gained significant attention in various scientific fields such as: (1) the study of drug discovery including deuterated drugs (heavy drugs), internal standards for bioanalysis, identification of metabolites, and quantitative proteomics[1−6]; (2) elucidation of life phenomena as tags, employing techniques such as Raman spectroscopy, magnetic resonance, and mass analysis[4,7−9]; (3) improving the functionality of materials to extend the lifespan of light-emitting diodes in organic electroluminescent devices[10]; (4) changing the properties of fragrance[11]; (5) and research regarding organic chemistry, such as the analysis of the reaction mechanism, and simplification of ^1H NMR, and protecting groups, utilizing the properties of stable C-D bonds.[1,12] Specifically, heavy drugs have gained considerable attention; for example, deutetrabenazine and deucravacitinib, which are prepared from commercially available CD_3 sources, were recently approved as heavy drugs by the Food and Drug Administration (Figure 1A). The deuterium switch (replacement of C-H bonds with C-D bonds) at the metabolic sites of drugs improves the bioavailability of mother drugs (H forms) owing to the deuterium kinetic isotope effect (KIE) and the stronger stability of C-D bonds than C-H bonds. Therefore, the development of practical deuteration protocols is highly significant and in high demand.

H/D exchange reactions are powerful and straightforward methods for the direct synthesis of deuterated compounds.[13−18] However, highly selective H/D exchange at the desired reaction sites in the presence of numerous reactive functional groups is difficult to achieve. Therefore, $LiAlD_4$ and $NaBD_4$ were used as reliable reductive deuteration reagents to incorporate deuterium atoms only at the metabolic sites of bioactive compounds for the study of drug discovery; however, these reagents are expensive and moisture-sensitive. In previous studies, 1-d_2-ethylamine ($CH_3CD_2NH_2$) and 1-d_2-phenethylamine ($PhCH_2CD_2NH_2$) were prepared from their corresponding nitrile substrates to synthesize deuterated bioactive compounds (Figure 1B).[19,20] Furthermore, sulfur (S)-containing molecules are highly significant owing to their versatile chemical properties, important bioactivities, and essential roles in various biological processes. For example, methionine, which bears a methylthio (S-Me) moiety, is a critical amino acid for growth and tissue repair in humans, and many S-containing substituents are present in bioactive compounds and peptide drugs.[21−24] Moreover, their deuterated forms have been utilized in various scientific fields. For example, homocysteine-ddhC-d_2, bearing deuterium atoms at the α-position of the S atom, was synthesized via the reductive deuteration of carboxylic acid using $NaBD_4$ and subsequent nucleophilic substitution using a thiol (Figure 1C).[25] The H/D exchange reaction at the α-thio C(sp^3)-H bonds was also reported using Ru/C under an expensive D_2 gas atmosphere at 60 °C for 3 days (Figure 1D).[26] This pioneer works can be applied to various substrates, including drugs. Because the S atom is known to poison transition metal catalysts, the deuteration efficiency was low, and a long reaction time was required; furthermore, the regioselectivity remained problematic. Therefore, the development of selective H/D exchange at the α-thio C(sp^3)-H bonds under metal-free conditions using an inexpensive deuterium source remains challenging and is eagerly desired, and the application to synthesis of the deuterated alkylating reagents[18], derived from deuterated products resulted by H/D exchange reaction, are also demanded.

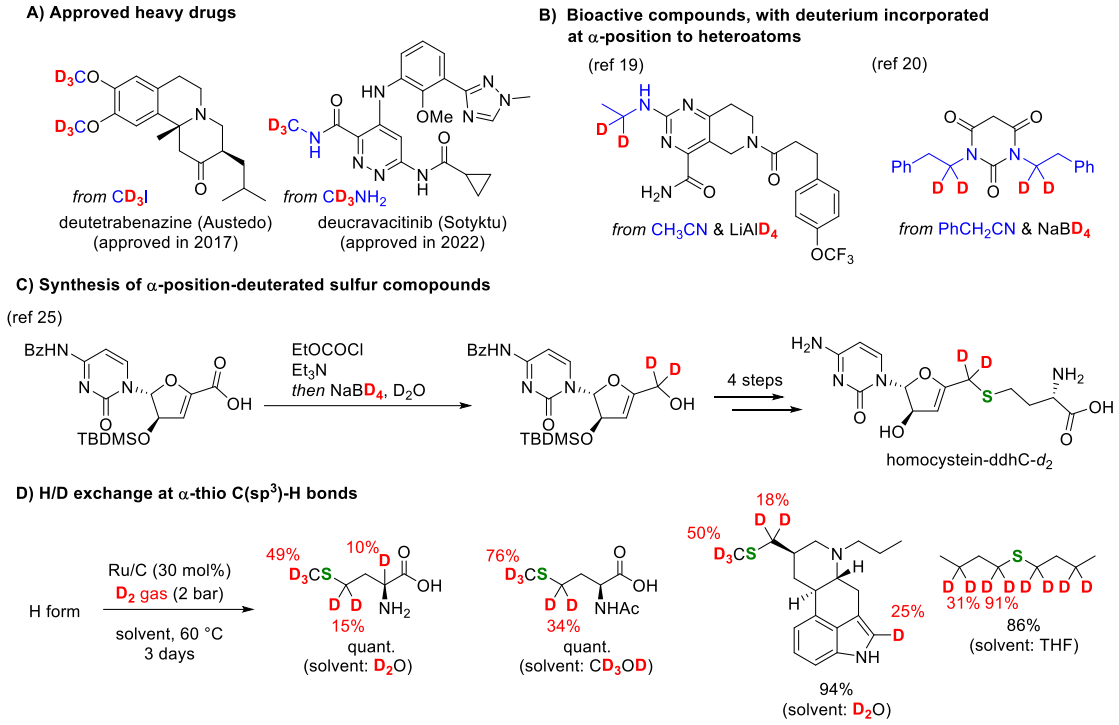

Figure 1. Utilization of deuterated compounds and their syntheses.

Photocatalytic H/D exchange at the C(sp³)-H bond is a valuable deuteration method considering the mild reaction conditions and good site-selectivity.[15] MacMillan developed the pioneering photocatalytic deuteration method at the α-amino C(sp³)-H bonds using 1,2,3,5-tetrakis(carbazol-9-yl)-4,6-dicyanobenzene (4CzIPN) as a photoredox catalyst in the presence of thiol and D_2O via a single electron transfer (SET) mechanism in 2017 (Figure 2A, left).[27] The deuterations of α-oxy C(sp³)-H bonds[28,29], α-amino C(sp³)-H bonds[29–32], formyl groups[33–36], and Si-H bonds[37] under photo-irradiation conditions were subsequently reported. In the substrate scope of the deuteration of formyl C-H bonds using tetrabutylammonium decataungstate (TBADT) as a hydrogen atom transfer (HAT) catalyst (Figure 2A, right), the deuteration of the α-position of the S atom on 4-(methylthio)benzaldehyde has been reported.[33] However, the deuteration efficiency of the methylthio group was moderate, and there was less selectivity between the formyl and methylthio groups. To address this, we investigated the photocatalytic and selective H/D exchange reaction of α-thio C(sp³)-H bonds using D_2O as an inexpensive deuterium source.

The choice of an appropriate photoredox catalyst[38,39] is important for achieving a highly regioselective deuteration via α-thio alkyl radicals generated from S-alkyl substrates[40–43] (Figure 2B). When using a HAT catalyst (e.g., TBADT[44–46]), the reaction sites generally depend on the difference in the bond dissociation energy (BDE) of the C-H bonds.[47] For example, 4-(methoxythio)anisole (**1**) is assumed to convert to **1**-d_6 resulting from the non-selective deuteration of methoxy and methylthio groups owing to the similar BDEs of α-thio C(sp³)-H (95.2 kcal/mol) and α-oxy C(sp³)-H (97.0 kcal/mol) (Figure 2B-1; our density functional theory (DFT) calculation is described in the Supporting Information, section 7). The BDE values (literature data[48]) also indicate that the selective deuteration of α-thio C(sp³)-H bonds in the presence of the benzylic position[49–51] and α-positions of O/N atoms[14,27,30–32] is difficult to achieve under HAT reaction conditions because there is no significant difference between their BDEs (Figure 2B-1, bottom). Alternatively, deuteration via the SET mechanism has the potential to achieve the desired selectivity for the deuteration of **1** to **1**-d_3 because the S atom is known to be more easily oxidized than the O atom (Figure 2B-2). For deuteration via the radical cation intermediate **C** generated via SET using a photoredox catalyst such as acridinium salt (Mes-Acr⁺ClO_4^-)[52] and dicyanoanthraquinone (DCA) as a one-electron oxidant, the deprotonation using the additional base is essential to form the radical intermediate **A**. These independent roles of SET and deprotonation, derived from each reagent, are assumed to reduce the efficiency of deuteration because **1** may be reproduced from **C** if the deprotonation step is not sufficiently fast. Conversely, we hypothesized that aromatic ketone photocatalysts can act as both, one-electron oxidants for the reaction of **1** to **C** and proton acceptors to facilitate the deprotonation (proton transfer (PT)) of **C** to **A**[42], and the subsequent incorporation of deuterium can provide the desired deuterated S-containing products. Based on these concepts, we developed a new highly selective H/D exchange reaction at the α-thio C(sp³)-H bonds without deuteration of the a-position of the O/N atoms, benzylic positions, or aromatic rings using thioxanthone- and anthraquinone-bearing aromatic ketone skeletons as organic photocatalysts[53] (Figure 2C). Additionally, the SET mechanism and applications for further transformation of the obtained deuterated products were elucidated.

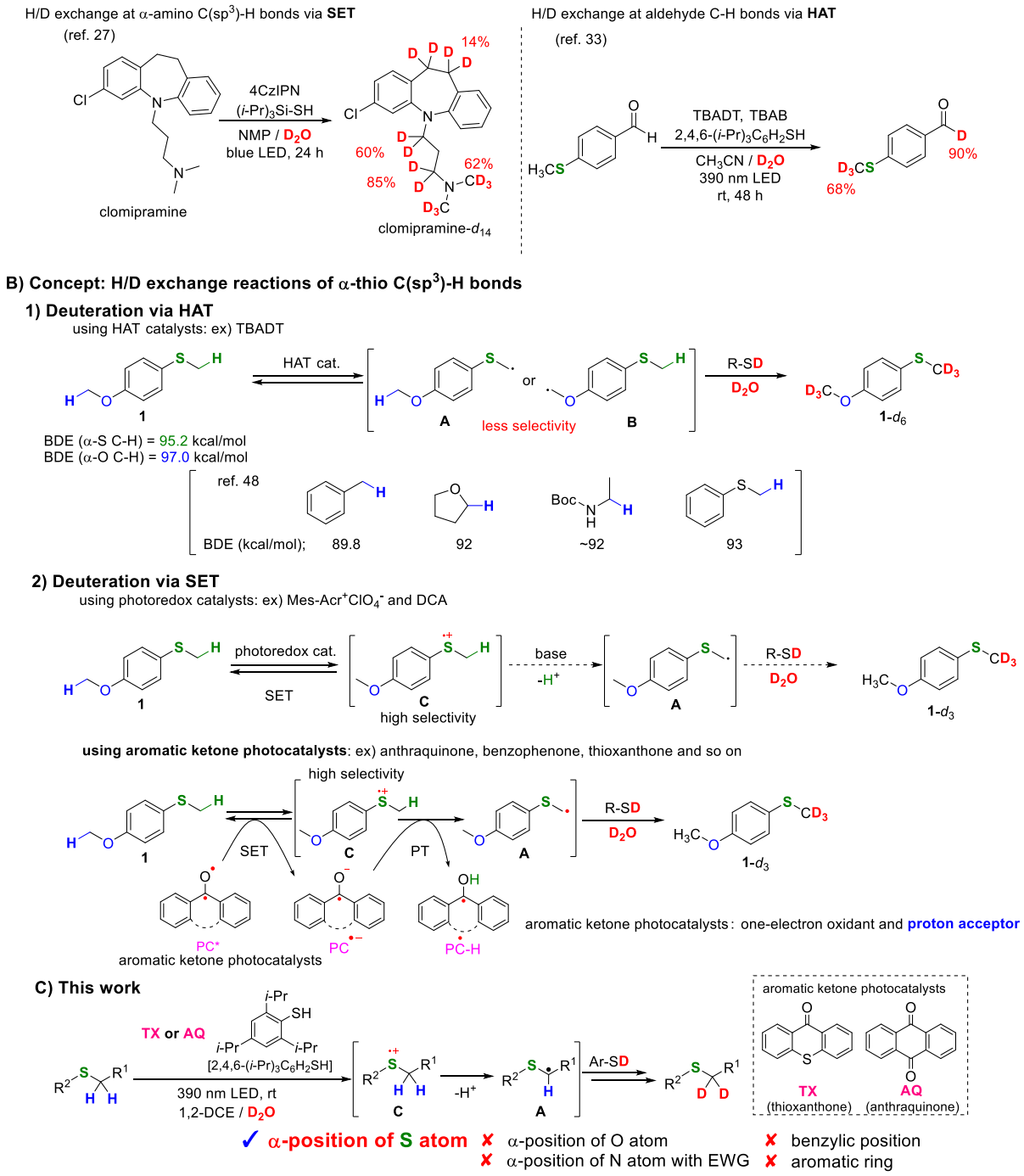

Figure 2. Concept of selective H/D exchange at α-thio C(sp³)-H bonds.

RESULTS AND DISCUSSION

Based on our concept (Figure 2B-2), the selective deuteration of 4-methoxythioanisole (**1**) as a model compound was successfully accomplished using aromatic ketone photocatalysts (PCs) in the presence of 2,4,6-triisopropylbenzene thiol (2,4,6-(*i*-Pr)$_3$C$_6$H$_2$SH) as a deuterium atom transfer (DAT) catalyst[27–35,37] in the mixed solvent of 1,2-dichloroethane (1,2-DCE) and D_2O under 390-nm irradiation (Figure 3, entries 1-5; details regarding optimization of the reaction conditions are described in the Supporting Information, Section 3). Screening of the aromatic ketone photocatalysts determined that thioxanthone (TX) was the most optimal catalyst providing the desired **1**-d_3 with an 85% yield, as well as 96% D content and perfect selectivity for the α-thio C(sp³)-H bonds after 24 h (entry 1). Anthraquinone (AQ) and benzophenone derivatives (BPs) were also suitable catalysts; however, their deuterium contents were moderate (entries 2-5). As expected (Figure 2B-1), the use of TBADT (E_{red}^* = ca. 2.44 V vs SCE)[54] as the HAT catalyst resulted in less selectivity with or without TBAB, and the deuterium content at the α-oxy C(sp³)-H bond was lower than that at the α-thio C(sp³)-H bond, depending on the difference in their BDEs (entries 6 and 7). The combination of the photoredox catalyst (Mes-Acr$^+$ClO$_4^-$ or DCA) and $NaHCO_3$ as a base gave no deuterated product (entries 8-10), likely because the reverse reaction of **C** to **1** was preferable for the deprotonation of **C** to **A** by the additional base (see Figure 2B-2). Additionally, the combination of DCA and TBAB was ineffective (entry

11). Under these reaction conditions, the cleavage of S-alkyl bond may occur as a side-reaction.[55] However, the corresponding byproducts (4-methoxythiophenol etc.) were not observed. The details of byproducts are not unclear.

				D contents (%)	
entry	PC (mol%)	LED (nm)	yield	a	b
1	TX	390	85%	0	96
2	AQ	390	68%	0	61
3	BP	390	94%	0	72
4	BP2	390	66%	0	43
5	BP3	390	79%	0	57
6[a,b]	TBADT	390	76%	11	42
7[a]	TBADT	390	86%	7	20
8[c]	Mes-Acr$^+$	456	0% (71% of **1** was recovered)		
9[c]	DCA	456	0% (77% of **1** was recovered)		
10[c]	DCA	456	0% (95% of **1** was recovered)		
11[b]	DCA	456	0% (74% of **1** was recovered)		

a) using 2 mol% of PC, b) using TBAB (20 mol%) as an additive
c) using $NaHCO_3$ (1.2 eq) as an additive

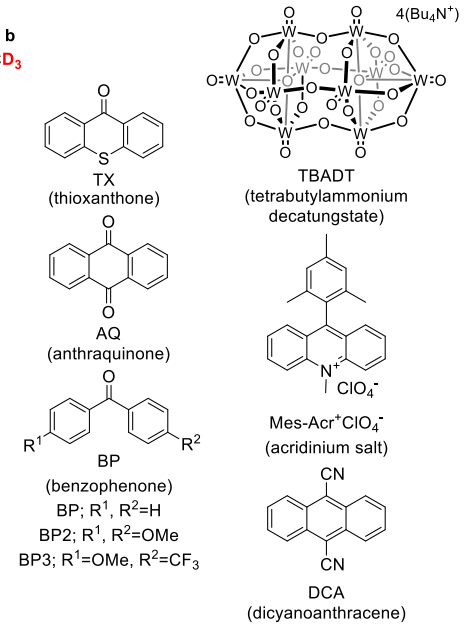

Figure 3. Screening of photocatalysts in the chemoselective H/D exchange reaction.

To further demonstrate the selectivity of our photocatalytic deuteration, a 1:1 mixture of thioanisole (**2**) and anisole (**3**) was used under the optimal reaction conditions. As a result, only thioanisole was deuterated, whereas anisole remained undeuterated, highlighting its excellent selectivity for H/D exchange at the α-thio C(sp^3)-H bonds (Figure 4A). Subsequently, the one-electron oxidation potentials of thioanisole and anisole were electrochemically determined to be E_{ox} = 1.36 and 1.67 V vs saturated calomel electrode (SCE), respectively (Figure 4B, see the details in the Supporting Information, Section 4). The one-electron reduction potential at the singlet excited state of thioxanthone (^{1}TX*; * denotes the excited state) was $^1E^*_{red} = E_{red} + {}^1E^*$ = 1.64 V vs SCE, as calculated from the one-electron reduction potential at the ground state (E_{red} = −1.55 V vs SCE) and the singlet excited energy ($^1E^* = [1/\lambda_{abs} + 1/\lambda_{fl}]/2$ = 3.19 eV) determined from experimental results of the absorption (λ_{abs} = 372 nm) and fluorescence maxima (λ_{fl} = 405 nm). The free-energy change of the photoinduced electron transfer from the thioanisole to the singlet excited state of thioxanthone was negative ($\Delta G_{et} = E_{ox} - {}^1E^*_{red}$ = −0.28 eV), indicating that SET is energetically feasible. In contrast, the electron transfer oxidation of thioanisole with the triplet excited state of thioxanthone ($^3E^*_{red}$ = 1.14 V vs SCE) is thermodynamically unfavored.

To clarify the details of the reaction mechanism, we examined the key intermediates via laser-induced time-resolved transient absorption spectroscopy (Figure 4C). Triplet–triplet absorption of TX in deaerated 1,2-DCE was observed at 640 nm[56,57] by nanosecond laser flash photolysis at 355 nm (Nd-YAG laser, FWHM = 10 ns) (Figure 4C-i). The transient absorption spectra in a 1,2-DCE solution containing TX and thioanisole (1.0 M) revealed the formation of TX radical anion (TX$^{\bullet-}$; λ_{max} = 360 nm[58]), and triplet excited state of TX (^{3}TX*) was observed at 640 nm (Figure 4C-ii). The TX radical anion, a unique intermediate formed via the SET mechanism, immediately appeared upon exposure to laser light at 360 nm, indicating that the photoinduced electron transfer from thioanisole to the singlet excited state of TX (^{1}TX*) occurred within nanoseconds, with a bimolecular rate constant of 10^8–10^{10} M^{-1} s^{-1} (The absorption band due to ^{1}TX* was not observed owing to its short lifetime).[59,60] Thus, the initial event of the photoinduced formation of the radical intermediate (**A**) is not HAT, but SET between the thioanisole and the singlet excited state of thioxanthone.[61,62]

Conversely, the decay rate-constant of ^{3}TX* observed at 640 nm was 2.24 x 10^6 s^{-1}, which is larger than the value in the absence of thioanisole (2.48 x 10^5 s^{-1}) (Figure 4C-i vs. 4C-ii). The bimolecular rate constant of the triplet excited state of TX with thioanisole was determined to be 2.0 × 10^6 M^{-1} s^{-1}, which indicated that it was significantly slower than the value of SET from thioanisole to ^{1}TX* (10^8–10^{10} M^{-1} s^{-1}). Thus, this photochemical reaction proceeds via the catalytic deprotonation pathway with singlet-sensitized SET rather than the triplet-sensitized HAT or proton-coupled electron transfer (PCET) pathway. To examine whether the triplet-sensitized proton transfer process at the α-thio C(sp^3)-H bonds influences the reaction rate, we conducted the KIE experiments using thioanisole-d_3 (PhSCD$_3$). Consequently, no significant KIE was observed (KIE (H/D) = 1.2) determined from the rate constants of electron-transfer from PhSCH$_3$ (2.0 × 10^6 M^{-1} s^{-1}) and PhSCD$_3$ (1.7 × 10^6 M^{-1} s^{-1}) to ^{3}TX* (Figures S9 and S10), which clearly supported that HAT and PCET pathways, where hydrogen abstraction is the rate-determining step, were unfavored. The bimolecular electron transfer from thioanisole to ^{3}TX* is thermodynamically unfavored due to the positive free energy (ΔG_{et} = +0.41 eV) as mentioned above. Electron transfer may occur in the exciplex with the strong interaction between thioanisole and ^{3}TX* to generate the radical ion pair.

The fluorescence of the ^{1}TX* was observed at 420 nm by the excitation (Figure S11). Upon addition of thioanisole, the emission intensity of TX slightly increased with increasing the thioanisole concentration (0 – 2.0 M). The broad emission band, obtained from the difference spectrum (Figure S11), was observed at around 500 nm probably due to the exciplex between ^{1}TX* and thioanisole. Electron transfer may occur in the exciplex to generate the radical ion pair, TX$^{\bullet-}$ and the radical cation of thioanisole. On the other hand, the fluorescence quenching of DCA with thioanisole was observed as shown in Figure S12. The electron-transfer rate constant was determined from the Stern-Volmer constant (26 M^{-1}) and the fluorescence lifetime (τ = 12 ns) to be 2.2 x 10^9 M^{-1} s^{-1}. No deuterated product was formed in the case of DCA-thioanisole system, fast back electron transfer from DCA$^{\bullet-}$ to the radical cation of thioanisole efficiently occur to form the original state as DCA and thioanisole (Figure 3, entry 10).[63]

In the proposed reaction mechanism, the photoexcitation of TX generates a singlet excited state of TX (^{1}TX*), which acts as a strong one-electron oxidant. Single electron transfer (SET) from thioanisole to

^{1}TX* in the exciplex occur to form a radical cation intermediate **C** accompanied by the radical anion of TX (TX$^{\bullet-}$) (Figure 4D). A subsequent PT between **C** and TX$^{\bullet-}$ produces the α-radical intermediate **A** and TX-H. Meanwhile, the thiol catalyst (Ar-SH) is considered to work as a DAT catalyst. The H/D exchange of Ar-SH with D_2O produces Ar-SD, which serves as the deuterium atom into **A** to produce the deuterated product. The TX catalyst is reproduced by SET and PT between TX-H and Ar-S$^{\bullet}$.

Radical clock experiments using the substrate **4**, bearing S-cyclopropylmethyl moiety, gave the ring-opened product **5**-d_1, which clearly indicated that the present deuteration proceeded via α-radical intermediate (Figure 4E).

A) Control experiments on the selectivity of H/D exchange between thioanisole 2 and anisole 3

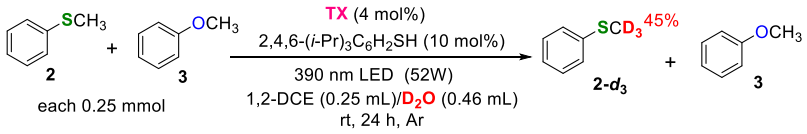

B) Oxidation potential of 2 and 3 and redction potential of thioxanthone

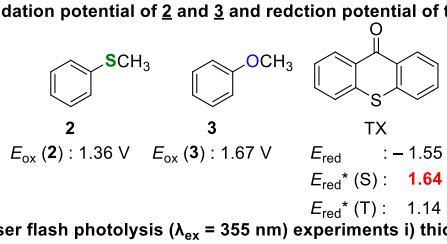

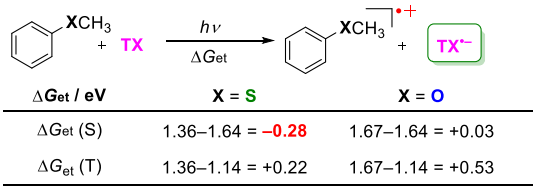

ΔGet / eV	X = S	X = O
ΔGet (S)	1.36–1.64 = –0.28	1.67–1.64 = +0.03
ΔGet (T)	1.36–1.14 = +0.22	1.67–1.14 = +0.53

C) Laser flash photolysis (λ_{ex} = 355 nm) experiments i) thioxanthone in 1,2-DCE ii) a mixture of thioxanthone and thioanisole in 1,2-DCE

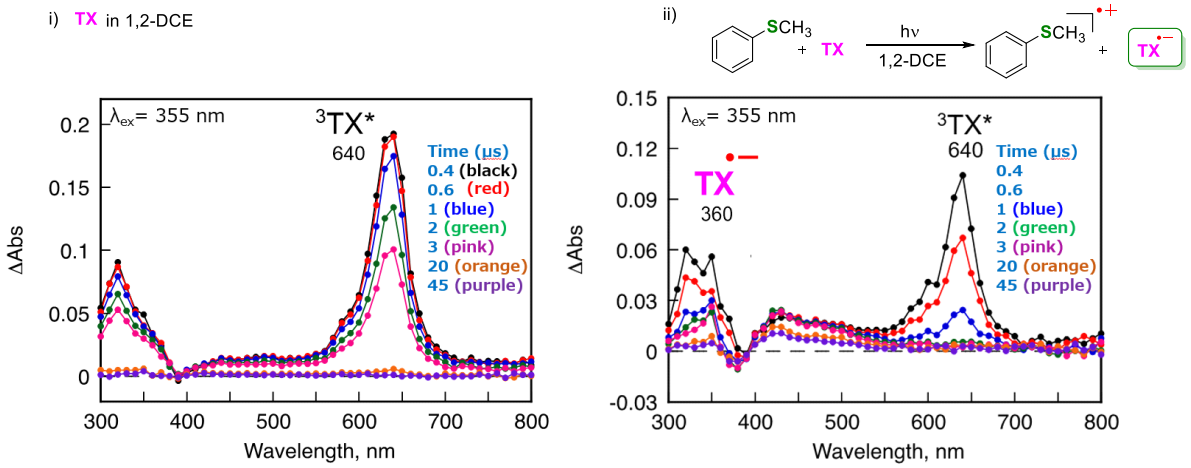

D) Proposed reaction mechanism

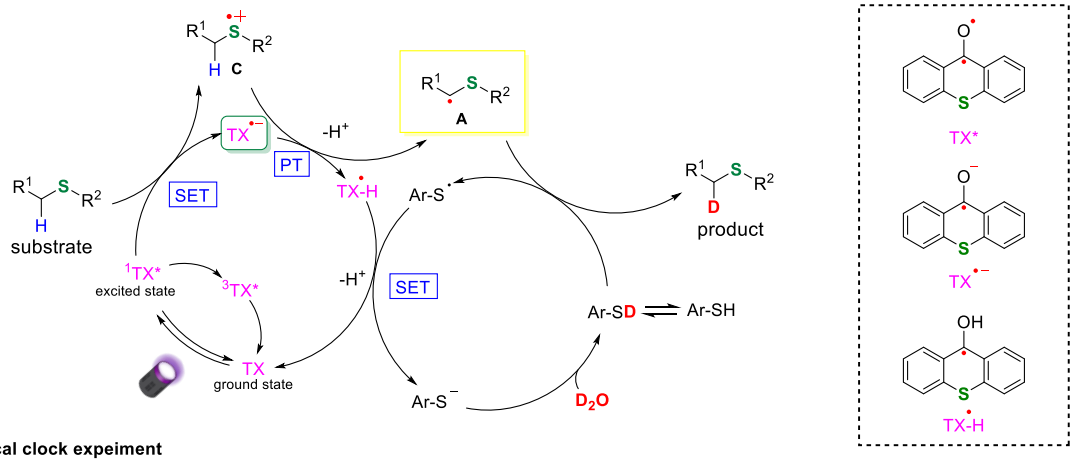

E) Radical clock expeiment

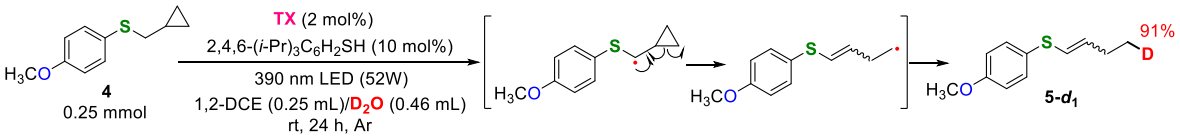

Figure 4. Mechanistic studies.

The substrate scope in the H/D exchange reactions at the α-thio C(sp^3)-H bonds was subsequently investigated (Figure 5); TX or AQ was used as the photocatalyst, resulting in the higher D contents (the deuteration efficiency depends on the combination of substrate and

catalyst, and details in the Supporting Information, Section 11). Various aryl alkyl sulfides (**6-16**; 4-Br-C_6H_4-, 4-MeO-C_6H_4-, phenyl, 2-pyridyl, 2-pyrimidinyl, 2-thiazyl as the aryl groups, and methyl, isopentyl, phenethyl, cyclopropyl, and isopropyl, etc. as the alkyl groups) underwent efficient deuteration with high selectivity at the α-thio Additionally, the methylene moieties of S,O-acetal (**17**) and S,S-acetal (**18**) were also deuterated. The present α-thio C(sp^3)-H bond-selective deuteration method was adapted to dialkyl sulfides (**19-23**) to produce the desired products, which were deuterated at two positions on the neighboring S atoms. Notably, the α-thio C(sp^3)-H bond-selective deuteration of **20-22** proceeded without deuteration of the α-position of N atom. Additionally, the α,β-unsaturated carbonyl moiety of **22** was tolerant under the present photocatalytic conditions. The α-thio C(sp^3)-H bond-selective deuteration of **23** could be accomplished without deuteration of the α-position of the ester because the present deuteration can proceed without an additional base (see Figure 2B). As illustrated in Figure 2A, the deuteration of 4-(methylthio)benzaldehyde (**24**) using TBADT was less selective and the deuteration efficiency of the formyl group was higher than that of the methylthio group. Meanwhile, the present photocatalytic method using AQ achieved a highly selective deuteration of the methylthio group of **24** demonstrating 68% D content, which was improved by repeated reactions to provide the desired deuterated product (**24**-d_3) with a high

C(sp^3)-H bonds without deuteration of the α-positions of the oxygen atom, benzylic positions, or aromatic rings. Note, deuteration of the substrates (**10** and **11**), bearing numerous α-oxy C(sp^3)-H bonds, was also applicable with a perfect selectivity at the α-thio C(sp^3)-H bonds.

D content (98% D)(The increase of photocatalyst and elongation of reaction time were also effective to get the higher D contents; see Table S4). Furthermore, a 1-g scale reaction of **1** was also applicable without any loss of D content (see Figure 3; entry 1). Various bioactive compounds could also undergo the present α-thio C(sp^3)-H bond-selective deuteration. Cysteine (**25**) and methionine (**26** and **27**) derivatives as S-containing amino acids were also applicable; note that the α-position of the selenium (Se) atom of the selenomethionine derivative (**28**) can be selectively deuterated in the same manner as the S atom. 1-Phenyl-1-thio-β-D-glucopyranoside tetraacetate (**29**) as the glucose derivative and the precursor of diltiazem (**30**) underwent deuterium incorporation while retaining its stereochemistry. For biotin derivative (**31**), the α-thio C(sp^3)-H bond deuteration proceeded with deuteration of the α-positions of the N atom. The low site-selectivity in the deuteration of **7** and **21** using TBADT clearly indicated that the present α-thio C(sp^3)-H bond-selective deuteration using TX and AQ via the SET mechanism can be a powerful tool for obtaining desirable deuterated S-containing products.

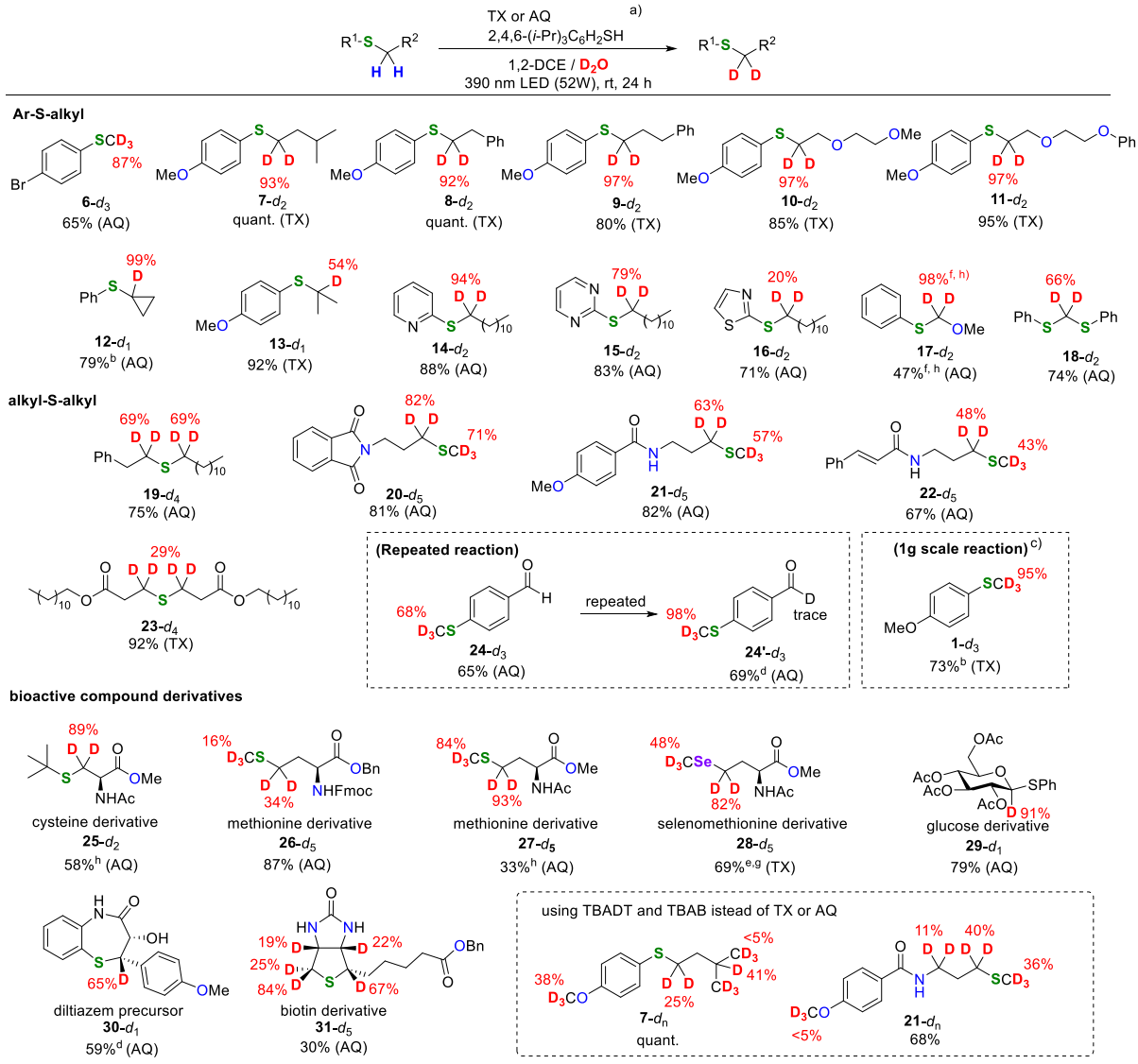

a) SM (0.25 mmol), TX or AQ (0.4 mol%), 2,4,6-(*i*-Pr)$_3$C$_6$H$_2$SH (10 mol%), 1,2-DCE (0.25 mL), D_2O (0.46 mmol, 25 mmol) were used. b) NMR yield. c) SM (6.5 mmol) was used. d) DCM was used instead of 1,2-DCE e) using 0.68 mL D_2O f) using 1.38 mL D_2O, g) repeated 2 times h) repeated 3 times

Figure 5. Substrate scope in the H/D exchange reactions of α-thio C(sp^3)-H bonds.

Finally, utilization of the obtained deuterated products for drug discovery and Raman spectroscopy was demonstrated. For drug discovery, the development of a preparation method (efficient introduction of the CD_3 moiety[64,65] and novel deuterated alkylating reagents[18,66] for drugs, bearing deuterium atoms at the α-position (metabolic sites) of oxygen and nitrogen atoms, is critical (Figure 1A–1C). **1**-d_3 was converted to CD_3-substituted diarylsulfonium salt (**32**-d_3) via *m*-chloroperoxybenzoic acid (*m*-CPBA) oxidation of the S atom and activation using triflic anhydride (Tf_2O); **32**-d_3 can be used as a CD_3-introducing reagent for phthalimide potassium salt to produce N-CD_3 phthalimide (**33**-d_3) without loss of the D content (Figure 6A-1). Furthermore, deuterated S,O-acetal **17**-d_2 can also act as a deuterated methylene source; namely, the reaction of 1,2-diol (**34**) with **17**-d_2 in the presence of 1,3-dibromo-5,5-dimethylhydantoin (DBDMH) and dibutylhydroxytoluene (HBT)[67] providing the 2,2-dideuterio-1,3-dioxolane product (**35**-d_2) with a high D content (Figure 6A-2). Additionally, **9**-d_2 and **11**-d_2 were used for the late-stage deuterated alkylation of the drugs (Figure 6A-3). The in-situ preparation of the deuterated alkyl iodides (D) from **9**-d_2 or **11**-d_2 using CH_3I under heating conditions[68] and the subsequent addition of sulfamethoxazole or ezetimibe produced the alkylated drugs (**36**-d_2–**39**-d_2), bearing deuterium atoms at the α-positions of the nitrogen or oxygen atoms with a high D content.

Deuterium labels have been used as Raman tags for biological species such as fatty acids[69], amino acids[70], sterols[71], and glucose[72], because deuterium labeling has a significantly limited effect on biological activities, and the C-D bond has a distinct vibrational frequency in the cell silent-region (1,800–2,700 cm^{-1}; range of wavenumbers where the Raman peaks from endogenous intracellular molecules such as proteins and lipids are not observed). For example, methionine-d_8 in its fully deuterated form (commercially available) can reportedly be used to observe the uptake of methionine (a fundamental amino acid essential for a wide range of biological processes, including protein synthesis, cancer metabolism, and epigenetics) in live HeLa cells via stimulated Raman scattering.[73] However, these deuterated analogs are expensive and tend to exhibit broad or complex spectra derived from different C-D bonds, limiting the simultaneous detection of several compounds. Several peaks were observed in the cell silent-region for methionine-d_8; however, the strongest Raman peak at 2127 cm^{-1} was used for specific imaging. We speculated that the methionine derivative developed in this study, **27**-d_5 (methionine derivative deuterated at the α-position of the S atom), would demonstrate a simpler Raman peak (DFT calculation of the Raman spectra of **27**-d_5 and its d_8- and d_3-analogues also supported this speculation; see Supporting Information, Section 14). A Raman analysis of **27**-d_5 demonstrated a peak at 2128 cm^{-1} whereas its non-deuterated analogue **27** did not show a peak in the cell silent-region (Figure 6B), indicating that deuteration at the α-thio C(sp^3)-H bonds is important for Raman imaging. These results also suggest that deuteration at the α-thio C(sp^3)-H bonds offers the simultaneous detection of several compounds with different C-D peaks or other Raman tags, such as alkyne- or nitrile-tags owing to the simpler spectrum and that deuterated agents for Raman imaging can be prepared efficiently and at a low cost using the method proposed in this study.

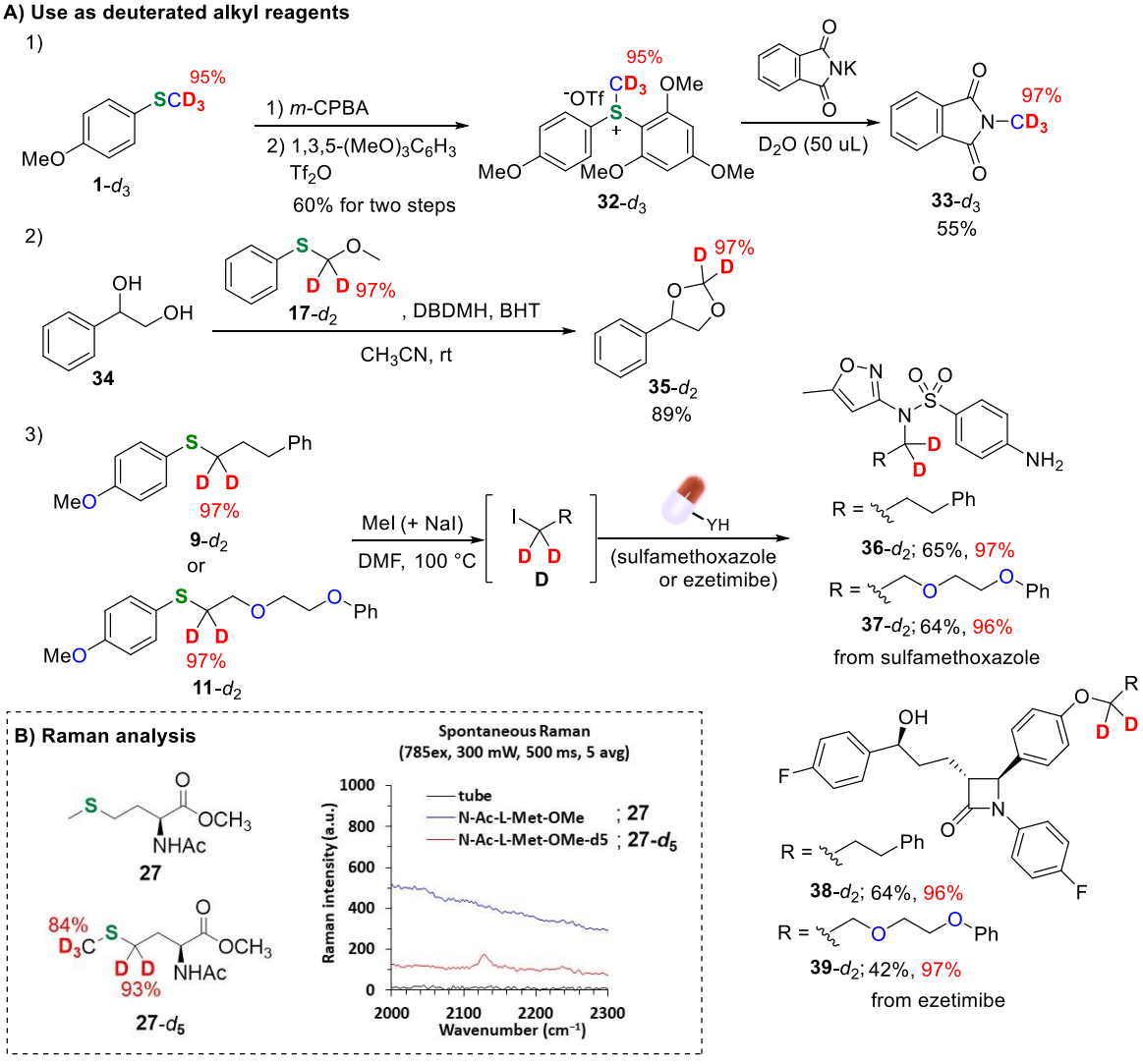

Figure 6. Application to further transformation of obtained deuterated products as deuterated alkyl reagents and Raman analysis of deuterated methionine derivative.

CONCLUSIIONS

We successfully developed a highly selective deuteration method at the α-positions of sulfur atoms using the thioxanthone or anthraquinone photocatalyst and D_2O as an inexpensive deuterium source. Importantly, the α-positions of the oxygen/nitrogen atoms, benzylic positions, and aromatic rings were not deuterated under the present reaction conditions. The SET reaction mechanism that achieves this unprecedented regioselectivity was elucidated using laser flash photolysis. This deuteration strategy applies to a range of sulfur-containing substrates, including pharmaceuticals and biologically relevant compounds. Furthermore, the deuterated products obtained by utilizing this method can provide novel deuterated alkylation reagents for future drug discovery and materials for Raman imaging applications. These advancements demonstrating the first use of thioxanthone and anthraquinone in photocatalytic deuteration have the potential for applications in various scientific and technological fields of deuterium.

ASSOCIATED CONTENT

Supporting Information. This material is available free of charge via the Internet at http://pubs.acs.org.
Cyclic voltammetry analyses for redox potential of thioanisole and anisole were shown on pages S6-S8. Emission spectroscopic data of thioxanthone was shown on page S9. Laser flash photolysis of solution of thioxanthone and thioanisole was shown on pages S10-S12. DFT calculation results were shown on pages S15-S23. Spectral data for all compounds and additional experimental details, materials, and methods, including photographs of the experimental setup were shown on pages S24-S59. Raman analysis of methionine derivative was shown on page S60-61. Spectra of substrates and products were shown on pages S66-S137 (PDF).

AUTHOR INFORMATION

Corresponding Author

* Yoshinari Sawama – Graduate School of Pharmaceutical Sciences, Osaka University 1-6 Yamada-oka, Suita, Osaka 565-0871, Japan Deuterium Science Research Unit, Center for the Promotion of Interdisciplinary Education and Research, Kyoto University, Yoshida, Sakyo-ku, Kyoto 606-8501, Japan. Email: sawama@phs.osaka-u.ac.jp

Author Contributions

The manuscript was written through the contributions of all authors.

Funding Sources

This study was supported by JSPS (MEXT grant in aid-for transformative research areas (B) Deuterium Science) KAKENHI Grant Number 20H05738 (for Y.S.), Grant-in-Aid for Scientific Research (B) KAKENHI Grant Number 24K01485 (for Y.S), Life Science and Drug Discovery (Basis for Supporting Innovative Drug Discovery and Life Science Research (BINDS)) from AMED under Grant Number 24ama121054 (for Y.S.), Takeda Science Foundation (for Y.S.), the Mochida Memorial Foundation for Medical and Pharmaceutical Research (for Y.S.), JST SPRING, Grant Number JPMJSP2138 (for M.M.), JST FOREST, Grant Number JPMJFR221M (for M.K.), Grant-in-Aid for Early-Career Scientists JP23K13709 (for Y. I.) and Grant-in-Aid for Challenging Research (Exploratory) JP24K21770 (for K.O.)

Notes

The authors declare no competing financial interest.

REFERENCES

(1) Gómez-Gallego, M.; Sierra, M. A. Kinetic isotope effects in the study of organometallic reaction mechanisms. *Chem. Rev.* **2011**, *111*, 4857–4963.

(2) Gant, T. G. Using deuterium in drug discovery: leaving the label in the drug. *J. Med. Chem.* **2014**, *57*, 3595–3611.

(3) Li, L.; Jakowski, J.; Do, C.; Hong, K. Deuteration and polymers: rich history with great potential. *Macromolecules* **2021**, *54*, 3555–3584.

(4) Atzrodt, J.; Derdau, V.; Kerr, W. J.; Reid, M. Deuterium- and tritium-labelled compounds: applications in the life sciences. *Angew. Chem. Int. Ed.* **2018**, *57*, 1758–1784.

(5) Di Martino, R. M. C.; Maxwell, B. D.; Pirali, T. Deuterium in drug discovery: progress, opportunities and challenges. N*at. Rev. Drug Discov.* **2023**, *22*, 562–584.

(6) Pirali, T.; Serafini, M.; Cargnin, S.; Genazzani, A. A. Applications of deuterium in medicinal chemistry. *J. Med. Chem.* **2019**, *62*, 5276–5297.

(7) Dodo, K.; Fujita, K.; Sodeoka, M. Raman spectroscopy for chemical biology research. *J. Am. Chem. Soc.* **2022**, *144*, 19651–19667.

(8) Serés Roig, E.; De Feyter, H. M.; Nixon, T. W.; Ruhm, L.; Nikulin, A. V.; Scheffler, K.; Avdievich, N. I.; Henning, A.; de Graaf, R. A. Deuterium Metabolic Imaging Of The Human Brain In Vivo At 7 T. *Magn. Reson. Med.* **2023**, *89*, 29–39.

(9) Takeo, E.; Fukusaki, E.; Shimma, S. Mass spectrometric enzyme histochemistry method developed for visualizing in situ cholinesterase activity in mus musculus and drosophila melanogaster. *Anal. Chem.* **2020**, *92*, 12379–12386.

(10) Yao, J.; Dong, S.-C.; Tam, B. S. T.; Tang, C. W. Lifetime Enhancement And Degradation Study Of Blue OLEDs using deuterated materials. *ACS Appl. Mater. Interfaces* **2023**, *15*, 7255–7262.

(11) Gane, S.; Georganakis, D.; Maniati, K.; Vamvakias, M.; Ragoussis, N.; Skoulakis, E. M. C.; Turin, L. Molecular vibration-sensing component in human olfaction. *PLoS One* **2013**, *8*, e55780.

(12) Miyashita, M.; Sasaki, M.; Hattori, I.; Sakai, M.; Tanino, K. Total synthesis of Norzoanthamine. *Science* **2004**, 305.

(13) Atzrodt, J.; Derdau, V.; Kerr, W. J.; Reid, M. C-H functionalisation for hydrogen isotope exchange. *Angew. Chem. Int. Ed.* **2018**, *57*, 3022–3047.

(14) Michelotti, A.; Roche, M. 40 Years of hydrogen–deuterium exchange adjacent to heteroatoms: A survey. *Synthesis (Mass.)* **2019**, *51*, 1319–1328.

(15) Zhou, R.; Ma, L.; Yang, X.; Cao, J. Recent Advances in Visible-Light Photocatalytic Deuteration Reactions. *Org. Chem. Front.* **2021**, *8*, 426–444.

(16) Prakash, G.; Paul, N.; Oliver, G. A.; Werz, D. B.; Maiti, D. C-H Deuteration of Organic Compounds and Potential Drug Candidates. *Chem. Soc. Rev.* **2022**, *51*, 3123–3163.

(17) Kopf, S.; Bourriquen, F.; Li, W.; Neumann, H.; Junge, K.; Beller, M. Recent developments for the deuterium and tritium labeling of organic molecules. *Chem. Rev.* **2022**, *122*, 6634–6718.

(18) Ogasahara, R.; Ban, K.; Mae, M.; Akai, S.; Sawama, Y. Deuterated alkyl sulfonium salt reagents; Importance of H/D exchange methods in drug discovery. *ChemMedChem* **2024**, *19*, e202400201.

(19) Sun, H.; Piotrowski, D. W.; Orr, S. T. M.; Warmus, J. S.; Wolford, A. C.; Coffey, S. B.; Futatsugi, K.; Zhang, Y.; Vaz, A. D. N. Deuterium isotope effects in drug pharmacokinetics II: Substrate-dependence of the reaction mechanism influences outcome for cytochrome P450 cleared drugs. *PLoS One* **2018**, *13*, e0206279.

(20) Xia, G.; Benmohamed, R.; Morimoto, R. I.; Kirsch, D. R.; Silverman, R. B. Deuteration and fluorination of 1,3-bis(2-phenylethyl)pyrimidine-2,4,6(1H,3H,5H)-trione to improve its pharmacokinetic properties. *Bioorg. Med. Chem. Lett.* **2014**, *24*, 5098–5101.

(21) Liu, Y.; Yu, Y.; Zhao, Q.; Tang, C.; Zhang, H.; Qin, Y.; Feng, X.; Zhang, J. Fluorescent probes based on nucleophilic aromatic substitution reactions for reactive sulfur and selenium species: Recent progress, applications, and design strategies. *Coord. Chem. Rev.* **2021**, *427*, 213601.

(22) Scott, K. A.; Njardarson, J. T. Analysis of us FDA-approved drugs containing sulfur atoms. *Top. Curr. Chem.* **2018**, *376*, 5.

(23) Liao, Y.; Wang, M.; Jiang, X. Sulfur-containing peptides: Synthesis and application in the discovery of potential drug candidates. *Curr. Opin. Chem. Biol.* **2023**, *75*, 102336.

(24) Feng, M.; Tang, B.; Liang, S. H.; Jiang, X. Sulfur containing scaffolds in drugs: Synthesis and application in medicinal chemistry. *Curr. Top. Med. Chem.* **2016**, *16*, 1200–1216.

(25) Wood, J. M.; Buckler, J. N.; Almo, S. C.; Evans, G. B.; Grove, T. L.; Harris, L. D. Synthesis of a putative ddhCTP metabolite ddhC-homocysteine. *Tetrahedron Lett.* **2023**, *119*, 154423.

(26) Gao, L.; Perato, S.; Garcia-Argote, S.; Taglang, C.; Martínez-Prieto, L. M.; Chollet, C.; Buisson, D.-A.; Dauvois, V.; Lesot, P.; Chaudret, B.; Rousseau, B.; Feuillastre, S.; Pieters, G. Ruthenium-catalyzed hydrogen isotope exchange of C(sp^3)-H bonds directed by a sulfur atom. *Chem. Commun.* **2018**, *54*, 2986–2989.

(27) Loh, Y. Y.; Nagao, K.; Hoover, A. J.; Hesk, D.; Rivera, N.; Colletti, S.; Davies, I.; MacMillan, D. Photoredox-catalyzed deuteration and tritiation of pharmaceutical compounds. *Science* **2017**, *358*, 1182–1187.

(28) Ogasahara, R.; Mae, M.; Matsuura, K.; Yoshimura, S.; Ishimoto, T.; Udagawa, T.; Harada, K.; Fujioka, H.; Kamiya, M.; Asada, R.; Uchiyama, H.; Tozuka, Y.; Akai, S.; Sawama, Y. Photocatalytic multiple deuteration of polyethylene glycol derivatives using deuterium oxide. *Chem. -Eur. J.* **2025**, *31*, e202404204.

(29) Meng, X.; Che, C.; Dong, Y.; Liu, Q.; Wang, W. Organophotocatalytic selective deuteration of metabolically labile heteroatom adjacent C-H bonds via H/D exchange with D_2O. *Org. Lett.* **2024**, *26*, 8961–8966.

(30) Meng, X.; Dong, Y.; Liu, Q.; Wang, W. Organophotocatalytic α-deuteration of unprotected primary amines via H/D exchange with D_2O. *Chem. Commun.* **2024**, *60*, 296–299.

(31) Legros, F.; Fernandez-Rodriguez, P.; Mishra, A.; Weck, R.; Bauer, A.; Sandvoss, M.; Ruf, S.; Méndez, M.; Mora-Radó, H.; Rackelmann, N.; Pöverlein, C.; Derdau, V. Photoredox-mediated hydrogen isotope exchange reactions of amino-acids, peptides, and peptide-derived drugs. *Chem. -Eur. J* **2020**, *26*, 12738–12742.

(32) Murugesan, K.; Donabauer, K.; Narobe, R.; Derdau, V.; Bauer, A.; König, B. Photoredox-catalyzed site-selective generation of carbanions from C(sp^3)–H bonds in amines. *ACS Catal.* **2022**, *12*, 3974–3984.

(33) Kuang, Y.; Cao, H.; Tang, H.; Chew, J.; Chen, W.; Shi, X.; Wu, J. Visible light driven deuteration of formyl C-H and hydridic C(sp^3)-H bonds in feedstock chemicals and pharmaceutical molecules. *Chem. Sci.* **2020**, *11*, 8912–8918.

(34) Zhang, Y.; Ji, P.; Dong, Y.; Wei, Y.; Wang, W. Deuteration of formyl groups via a catalytic radical H/D exchange approach. *ACS Catal.* **2020**, *10*, 2226–2230.

(35) Dong, J.; Wang, X.; Wang, Z.; Song, H.; Liu, Y.; Wang, Q. Formyl-selective deuteration of aldehydes with D_2O via synergistic organic and photoredox catalysis. *Chem. Sci.* **2019**, *11*, 1026–1031.

(36) Xu, Q.; Ou, W.; Hou, H.; Wang, Q.; Yu, L.; Su, C. Photosynthesis of C-1-deuterated aldehydes via chlorine radical-mediated selective deuteration of the formyl C-H bond. *Org. Lett.* **2024**, *26*, 4098–4103.

(37) Zhou, R.; Li, J.; Cheo, H. W.; Chua, R.; Zhan, G.; Hou, Z.; Wu, J. Visible-light-mediated deuteration of silanes with deuterium oxide. *Chem. Sci.* **2019**, *10*, 7340–7344.

(38) Nicewicz, D.; Roth, H.; Romero, N. Experimental and calculated electrochemical potentials of common organic molecules for applications to single-electron redox chemistry. *Synlett* **2015**, *27*, 714–723.

(39) Di Terlizzi, L.; Nicchio, L.; Protti, S.; Fagnoni, M. Visible photons as ideal reagents for the activation of coloured organic compounds. *Chem. Soc. Rev.* **2024**, *53*, 4926–4975.

(40) Le, C.; Liang, Y.; Evans, R. W.; Li, X.; MacMillan, D. W. C. Selective sp^3 C-H alkylation via polarity-match-based cross-coupling. *Nature* **2017**, *547*, 79–83.

(41) Kim, J.; Li, B. X.; Huang, R. Y.-C.; Qiao, J. X.; Ewing, W. R.; MacMillan, D. W. C. Site-selective functionalization of methionine residues via photoredox catalysis. *J. Am. Chem. Soc.* **2020**, *142*, 21260–21266.

(42) Knowles, O. J.; Johannissen, L. O.; Crisenza, G. E. M.; Hay, S.; Leys, D.; Procter, D. J. A Vitamin B_2 -photocatalysed approach to methionine analogues. *Angew. Chem. Int. Ed.* **2022**, *61*, e202212158.

(43) Tan, Z.; Zhu, S.; Liu, Y.; Feng, X. Photoinduced chemo-, site- and stereoselective α-C(sp^3)-H functionalization of sulfides. *Angew. Chem. Int. Ed.* **2022**, *61*, e202203374.

(44) Ravelli, D.; Fagnoni, M.; Fukuyama, T.; Nishikawa, T.; Ryu, I. Site-selective C–H functionalization by decatungstate anion photocatalysis: Synergistic control by polar and steric effects expands the reaction scope. *ACS Catal.* **2018**, *8*, 701–713.

(45) Laudadio, G.; Deng, Y.; van der Wal, K.; Ravelli, D.; Nuño, M.; Fagnoni, M.; Guthrie, D.; Sun, Y.; Noël, T. C(sp^3)–H functionalizations of light hydrocarbons using decatungstate photocatalysis in flow. *Science* **2020**, *369*, 92–96.

(46) Hong, B.-C.; Indurmuddam, R. R. Tetrabutylammonium decatungstate (TBADT), a compelling and trailblazing catalyst for visible-light-induced organic photocatalysis. *Org. Biomol. Chem.* **2024**, *22*, 3799–3842.

(47) Capaldo, L.; Ravelli, D. Direct photocatalyzed hydrogen atom transfer (HAT) for aliphatic C–H bonds elaboration. *Chem. Rev.* **2022**, *122*, 1875–1924.

(48) Y.-R. Luo, *Handbook of bond dissociation energies in organic compounds*, CRC Press: Boca Raton, FL, **2002**.

(49) Du, H.-Z.; Fan, J.-Z.; Wang, Z.-Z.; Strotman, N. A.; Yang, H.; Guan, B.-T. Cesium amide-catalyzed selective deuteration of benzylic C-H bonds with D_2 and application for tritiation of pharmaceuticals. *Angew. Chem. Int. Ed.* **2023**, *62*, e202214461.

(50) Grotjahn, S.; Graf, C.; Zelenka, J.; Pattanaik, A.; Müller, L.; Kutta, R. J.; Rehbein, J.; Roithová, J.; Gschwind, R. M.; Nuernberger, P.; König, B. Reactivity of superbasic carbanions generated via reductive radical-polar crossover in the context of photoredox catalysis. *Angew. Chem. Int. Ed.* **2024**, *63*, e202400815.

(51) Grotjahn, S.; Müller, L.; Pattanaik, A.; Falk, A.; Barison, G.; Bauer, J. O.; Rehbein, J.; Gschwind, R. M.; König, B. Regio-, diastereo- and enantioselectivity in the photocatalytic generation of carbanions via hydrogen atom transfer and reductive radical-polar crossover. *Org. Chem. Front.* **2024**, *11*, 5890–5900.

(52) Fukuzumi, S.; Kotani, H.; Ohkubo, K.; Ogo, S.; Tkachenko, N. V.; Lemmetyinen, H. Electron-transfer state of 9-mesityl-10-methylacridinium ion with a much longer lifetime and higher energy than that of the natural photosynthetic reaction center. *J. Am. Chem. Soc.* **2004**, *126*, 1600–1601.

(53) Romero, N. A.; Nicewicz, D. A. Organic photoredox catalysis. *Chem. Rev.* **2016**, *116*, 10075–10166.

(54) Waele, V. D.; Poizat, O.; Fagnoni, M.; Bagno, A.; Ravelli, D. Unraveling the key features of the reactive state of decatungstate anion in hydrogen atom transfer (HAT) photocatalysis. *ACS Catal.* **2016**, *6*, 7174–7182.

(55) Baciocchi, E.; Del Giacco, T.; Gerini, M. F.; Lanzalunga, O. Rates of C-S bond cleavage in tert-alkyl phenyl sulfide radical cations. *Org. Lett.* **2006**, *8*, 641–644.

(56) Wöll, D.; Laimgruber, S.; Galetskaya, M.; Smirnova, J.; Pfleiderer, W.; Heinz, B.; Gilch, P.; Steiner, U. E. On the mechanism of intramolecular sensitization of photocleavage of the 2-(2-nitrophenyl)propoxycarbonyl (NPPOC) protecting group. *J. Am. Chem. Soc.* **2007**, *129*, 12148–12158.

(57) Mundt, R.; Villnow, T.; Ziegenbein, C. T.; Gilch, P.; Marian, C.; Rai-Constapel, V. Thioxanthone in apolar solvents: Ultrafast internal conversion precedes fast intersystem crossing. *Phys. Chem. Chem. Phys.* **2016**, *18*, 6637–6647.

(58) Allen, N. S.; Catalina, F.; Green, P. N.; Green, W. A. Photodegradation and photostabilisation of polymers: Synergistic effects of light stabilizers, *Eur. Polym. J.* **1985**, *21*, 841.

(59) Angulo, G.; Grilj, J.; Vauthey, E.; Serrano-Andrés, L.; Rubio-Pons, O.; Jacques, P. Ultrafast decay of the excited singlet states of thioxanthone by internal conversion and intersystem crossing. *ChemPhysChem* **2010**, *11*, 480–488.

(60) Nikitas, N. F.; Gkizis, P. L.; Kokotos, C. G. Thioxanthone: A powerful photocatalyst for organic reactions. *Org. Biomol. Chem.* **2021**, *19*, 5237–5253.

(61) The absorption band due to TX˙-H (l = 410 nm) is overlapped with the absorption bleaching due to the ground state of TX. See; Rodrigues, J. F.; Silvaa, F. d. A. d.; Netto-Ferreira, J. C. Photochemical reactivity of thioxanthone: A time-resolved study in homogeneous and heterogeneous systems. *J. Braz. Chem. Soc.* **2010**, *21*, 960–965.

(62) Thioanisole radical cation was detectable at 470 nm as the dimer radical cation, being associated with a large excess of thioanisole (1.0 M). This absorption is overlapped with the other transient species. See; Yokoi, H.; Hatta, A.; Ishiguro, K.; Sawaki, Y. Formation of σ- and π-type dimer radical cations by the photochemical one-electron oxidation of aromatic sulfides. *J. Am. Chem. Soc.* **1998**, *120*, 12728–12733.

(63) The deuteration using AQ and BP as photosensitizer may proceed via the different reaction mechanism.

(64) Wang, M.; Zhao, Y.; Zhao, Y.; Shi, Z. Bioinspired design of a robust d_3-methylating agent. *Sci. Adv.* **2020**, *6*, eaba0946.

(65) Chen, J.; Liu, S.; Su, S.; Fan, R.; Zhang, R.; Meng, W.; Tan, J. Sulfonium-based precise alkyl transposition reactions. *Sci. Adv.* **2023**, *9*, eadi1370.

(66) Ban, K.; Imai, K.; Oyama, S.; Tokunaga, J.; Ikeda, Y.; Uchiyama, H.; Kadota, K.; Tozuka, Y.; Akai, S.; Sawama, Y. Sulfonium salt reagents for the introduction of deuterated alkyl groups in drug discovery. *Angew. Chem. Int. Ed.* **2023**, *62*, e202311058.

(67) Maegawa, T.; Koutani, Y.; Otake, K.; Fujioka, H. Methylene acetal formation from 1,2- and 1,3-diols using an O,S-acetal, 1,3-dibromo-5,5-dimethylhydantoin, and BHT. *J. Org. Chem.* **2013**, *78*, 3384–3390.

(68) Mamalis, P. Reaction of some substituted methylthiomethyl-benzenes and -naphthalenes with methyl iodide. *J. Chem. Soc.* **1960**, 4747–4753.

(69) Zhang, D.; Slipchenko, M. N.; Cheng, J.-X. Highly sensitive vibrational imaging by femtosecond pulse stimulated Raman loss. *J. Phys. Chem. Lett.* **2011**, *2*, 1248–1253.

(70) Wei, L.; Yu, Y.; Shen, Y.; Wang, M. C.; Min, W. Vibrational imaging of newly synthesized proteins in live cells by stimulated Raman scattering microscopy. *Proc. Natl. Acad. Sci. U. S. A.* **2013**, *110*, 11226–11231.

(71) Alfonso-García, A.; Pfisterer, S. G.; Riezman, H.; Ikonen, E.; Potma, E. O. D_{38}-cholesterol as a Raman active probe for imaging intracellular cholesterol storage. *J. Biomed. Opt.* **2016**, *21*, 61003.

(72) Li, J.; Cheng, J.-X. Direct visualization of de novo lipogenesis in single living cells. *Sci. Rep.* **2014**, *4*, 6807.

(73) Spratt, S. J.; Oguchi, K.; Miura, K.; Asanuma, M.; Kosakamoto, H.; Obata, F.; Ozeki, Y. Probing methionine uptake in live cells by deuterium labeling and stimulated Raman scattering. *J. Phys. Chem. B* **2022**, *126*, 1633–1639.

the Table of Contents (TOC)